

Crystallization and isothermal thickening of single crystals of $C_{246}H_{494}$ in dilute solution

J.K. Hobbs*, M.J. Hill, P.J. Barham

University of Bristol, H.H. Wills Physics Laboratory, Tyndall Avenue, Bristol BS8 1TL, UK

Received 17 October 1999; received in revised form 22 May 2000; accepted 13 June 2000

Abstract

Crystals of the uniform, long alkane $C_{246}H_{494}$ have been grown from dilute solution in extended chain and a number of integer folded forms, following our earlier work on solution crystallization and thickening of $C_{294}H_{590}$ and $C_{198}H_{398}$. Crystallization rates have been measured using DSC, and minima in growth rates found at both the transition between primary growth in the twice-folded (2F) and once-folded (1F) forms, and at the transition between primary growth in the 1F and extended (E) forms. Isothermal thickening has been followed both in the DSC and by TEM examination of the resultant crystal morphologies; allowing direct correlations to be made between the thickening kinetics and the changes in morphology. Different modes of thickening have been observed depending on the particular integer folded forms studied. Thickening between 2F and 1F crystals is accompanied by screw dislocation growth at crystal edges, and appears to occur largely through a solid state process resulting in a small scale roughness. Thickening between 1F and E crystals is likewise accompanied by screw dislocation growth at crystal edges but appears to proceed, at least partially, through a larger scale re-organization resulting in small, crystallographic, lozenge shaped, multiple twins. Differences between the thickening behaviour observed when samples are prepared in the DSC (using aluminium pans) or in oil baths (using glass tubes) are also discussed. © 2000 Elsevier Science Ltd. All rights reserved.

Keywords: *n*-Alkanes; Isothermal thickening; Crystallization

1. Introduction

The recent availability of a new supply of ultra-long alkanes in gram quantities [1] has allowed us to revisit the question of isothermal thickening in solution, originally studied in $C_{198}H_{398}$ [2,3]. In that work the thickening of once-folded crystals into the extended form was studied in separate experiments using differential scanning calorimetry (DSC) and transmission electron microscopy (TEM). A range of morphologies associated with thickening were observed but could not be directly correlated with the rate data from DSC as the concentrations were considerably different. The increased quantities of material now available have allowed both the study of different chain lengths and a more rigorous approach to be taken to the matching of the crystal morphologies, thermal behaviour as studied by DSC, and crystal thickening found through Raman LAM and SAXS. In this work we have grown crystals in fairly dilute solution ($\sim 0.2\%$ w/w) in DSC pans, characterized their crystallization rates and

transformation rates, and then harvested the crystals at predetermined points during their transformation, so that the relationship between the crystal morphology and the dissolution behaviour is known.

In this paper we address the crystallization and isothermal thickening of solution grown crystals of $C_{246}H_{494}$, thickening between once-folded and extended forms, and twice-folded and once-folded forms. An introduction to the background to isothermal thickening in ultra-long alkanes and its relevance to the behaviour found in polyethylene is given in a previous paper [4] in which we reported the thickening behaviour of the longer alkane $C_{294}H_{590}$. In that previous paper we were only able to access the thickening behaviour between the different folded forms of the longer alkane, whereas previous studies of $C_{198}H_{398}$ [2] had primarily dealt with thickening between once-folded (1F) and extended (E) forms. In the present work we have been able to bridge the gap between these two different modes of thickening while maintaining the rigorous connection with DSC characterization developed for $C_{294}H_{590}$ [4].

2. Experimental

The materials used in this study were kindly provided by

* Corresponding author. Tel.: +44-117-9288747; fax: +44-117-9255624.

E-mail address: jamie.hobbs@bristol.ac.uk (J.K. Hobbs).

G. Brooke [1] and the Engineering and Physical Science Research Council (EPSRC).

Two different sample preparation techniques for subsequent study by TEM were used. For most of the morphologies presented here, where comparison with results from DSC was required, samples were prepared in the DSC. A Perkin–Elmer DSC7 was used. For each sample, approximately 0.02 mg of $C_{246}H_{494}$ was weighed into an aluminium DSC pan suitable for volatile liquids, approximately 7 mg of toluene was added and the pan sealed, to give a sample concentration in the range 0.1–0.4% w/w (all subsequent concentrations quoted will be % w/w). The sample was then heated to 110°C, cooled immediately to 105°C and held for 1 min to ensure that the alkane was completely dissolved, cooled to the selected crystallization temperature, and allowed to crystallize for a given length of time. The sample was then re-heated in the DSC, the resultant dissolution endotherm allowing the extent of crystallization and the form of the crystals (e.g. once-folded, extended etc.) to be determined in the same manner as had been used previously in this laboratory for the study of crystallization rates [5,6,7]. The process was then repeated, but the sample was not heated from the crystallization temperature but rather quenched to room temperature at the maximum cooling rate of the DSC ($\sim 40^\circ/\text{min}$).

In some instances a further check was performed to ascertain how much further crystallization occurred on cooling to room temperature. The quenched sample was re-dissolved at a heating rate of $20^\circ\text{C}/\text{min}$ (a rate which has previously been found to prevent most rearrangement of the sample [6]). The amount of additional crystallization could then be found from the difference in the melting endotherms of the quenched and unquenched samples.

Once the sample was fully characterized and crystallized in the desired form, the DSC pan was removed from the DSC, cut open with a scalpel and shaken vigorously in excess toluene (approximately 0.5 ml) in order to remove the crystals from the DSC pan. A drop of the resulting suspension was then placed onto a carbon covered TEM grid, shadowed with platinum palladium and viewed with a Phillips 400 TEM.

The method described above for preparing samples sometimes resulted in somewhat damaged crystals as it requires vigorous shaking of the pan in toluene. Also, only very small amounts of material could be prepared in this way due to the small sample volume of the DSC pans and the requirement to use low concentrations. Therefore, at some crystallization temperatures, large quantities of crystal were prepared using more standard sample preparation techniques. In these cases crystals were grown in glass tubes in oil baths. Samples of $C_{246}H_{494}$ were placed into the glass tubes, toluene added to a concentration of approximately 0.2% w/w and the glass tubes flame sealed to prevent escape of toluene during crystallization. Each sample was heated in an oil bath at 105°C for 5 min to dissolve the alkane in the toluene, and then transferred to a second, preheated oil bath

at the desired crystallization temperature, where it was held isothermally for the desired crystallization time. The tube was then removed from the oil bath, broken open, and the resulting suspension prepared for study by TEM as described above. It was found that the nucleation rates of these samples prepared in oil baths using glass tubes, were considerably slower than those of samples prepared in the DSC using aluminium pans, so total crystallization times were not easily comparable. For this reason, as the intention of this study was direct comparison between morphology and DSC data, the majority of samples were prepared in the DSC.

It was possible to calculate the rate of crystallization from the DSC in direct comparison with previous work on $C_{246}H_{494}$ using higher concentrations [6]. The same technique as described in Ref. [5] was used, in which a crystallization curve is built up from successive isothermal crystallization and dissolution runs. The sample is crystallized for a given length of time, dissolved directly from the crystallization temperature and the area of the resultant endotherm measured. The process is repeated for different lengths of time at the same crystallization temperature until an Avrami type rate curve of endotherm area vs. time has been built up, from which an approximate growth “rate”, the tangent to the steepest part of the curve, can be determined. This technique was used for a single sample of $C_{246}H_{494}$ with a concentration of 0.14% w/w, which can be taken as representative of the concentration range under study here. It was only possible to measure rates unambiguously at crystallization temperatures down to 71°C , as below this temperature crystallization was prohibitively fast, and the unambiguous identification of the crystal form was not possible from the DSC trace as further discussed in Section 3. Times described as “onset” times (which should be closely related to the nucleation rates) were also estimated by extrapolating the tangent to the endotherm area vs. time curve to zero area.

3. Results and discussion

In this paper we present three separate but interconnected sets of data: the results of a DSC study of the crystallization rates of a dilute solution of $C_{246}H_{494}$; the morphologies of $C_{246}H_{494}$ that occur on primary crystallization from dilute solution in glassware in oil baths; and the morphologies found during and after isothermal thickening of $C_{246}H_{494}$ in solution along with their corresponding DSC behaviour.

3.1. Crystallization rates

In this section we present the results of a DSC study of the crystallization of a single sample of $C_{246}H_{494}$ from dilute solution (using a concentration of 0.14% w/w).

Fig. 1a shows the variation in crystallization rate with crystallization temperature. Fig. 1b shows the variation in onset of crystallization with temperature. At the lowest

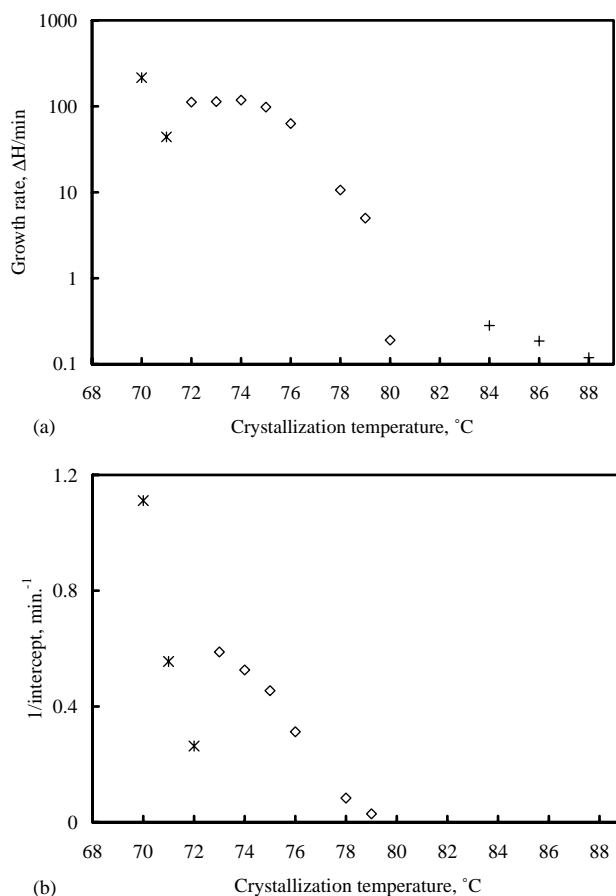


Fig. 1. (a) A graph showing the variation in crystallization rate with crystallization temperature for a 0.14% w/w solution of C₂₄₆H₄₉₄ in toluene. (b) A graph showing the variation with crystallization temperature of the reciprocal of the intercept time. The intercept time is the time at which the endotherm area vs. crystallization time curve extrapolates to zero endotherm area, using the linear part of the sigmoidal curve to make the extrapolation. The different symbols refer to primary growth in the different forms: (X), primary growth in the 2F form; (◇), primary growth in the 1F form; and (+), primary growth in the E form.

temperatures (70–72°C) the initial structure, after very short times, is 2F which rapidly rearranges to the 1F form. We have included the areas of both 2F and 1F material in this calculation of the growth rates as, at short times, it appears that most of the 1F material seen to dissolve in the DSC has come from rearrangement on heating. It is very clear that the crystallization rate passes through two minima, one at approximately 71°C and the other between 80 and 84°C. At temperatures in between 80 and 84°C the growth rates were found to be too slow to allow study over reasonable time periods. The onset of crystallization is only shown at temperatures up to 79°C, above this temperature the crystallization rate was so slow that unacceptably large errors are introduced into the onset time. It is apparent that there is also a minimum in the onset time, this time at 72°C. Fig. 2 shows a series of isothermal crystallization curves for the sample recorded in Fig. 1, from which it can be seen that crystallization is substantially slower in the temperature

range 71–72°C than it is both above and below these temperatures. The data for the sample crystallized at 71°C appears different from the rest in that the heat flow does not pass through a clear minimum but rather drops to a lower level and then stays there. We do not have an explanation for this unusual behaviour — the heat flow does not return to the expected higher level even after longer holding times.

The observation of growth rate minima as the crystallization temperature is lowered is in agreement with previous observations on other strictly uniform alkanes [5–10]. However, in this study we have, for the first time, observed two minima in the same chain length alkane and in the same sample, one between E and 1F and another between 1F and 2F forms. The very clear presence of a minimum in overall rate can be seen from the isothermal enthalpy data; crystallization occurs both more slowly, and after a longer gestation time, at 72°C than at both 70 and 73°C. The “growth rate” minimum between 2F and 1F growth occurs slightly below the temperature at which primary growth is first seen in the 2F form. While the “nucleation minimum” falls at 72°C, the temperature where primary growth is first seen in the 2F form.

The growth rate minimum that occurs between the primary growth of material in the 1F and E forms is

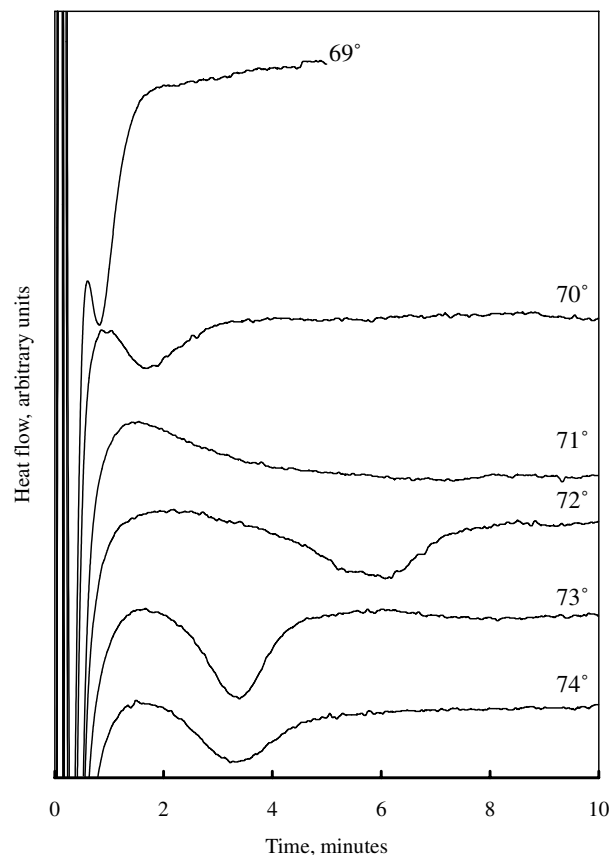


Fig. 2. A series of crystallization exotherms obtained during isothermal crystallization at different crystallization temperatures. The crystallization temperatures are marked on each curve.

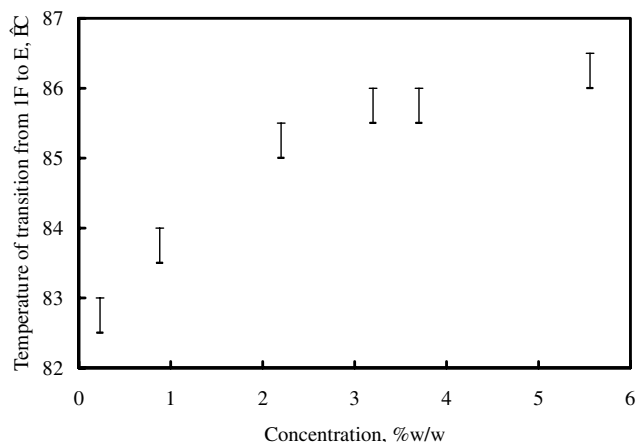


Fig. 3. The variation with sample concentration of the temperature at which the transition from primary growth in the 1F form to primary growth in the extended form occurs in $C_{246}H_{494}$. The lower limit of the “error bars” show the highest temperature at which the 1F form was observed, the upper limit shows the lowest temperature at which primary growth was observed in the extended form.

unusually broad. As we are using very low concentrations, in which crystal growth is substantially slower than that seen in higher concentrations, we did not attempt to define the precise temperature at which growth occurred most slowly. It is, however, striking that the crystallization rate at 84°C is faster than that at 80°C. This is in agreement with a previous study of solution crystallization of $C_{246}H_{494}$ in this laboratory [6] in which it was found that crystallization at 88°C occurred more rapidly than at 84°C. The fact that the absolute value of the minimum has apparently moved to lower temperatures is because of the change in concentration (0.14% w/w compared with 1.1% w/w) as discussed below.

Fig. 3 shows the relationship between the temperature at which crystal growth was first seen in the once folded form and the solution concentration. Here the “error” bars show the range of temperatures over which the transition from 1F to E growth occurs; the high temperature of the bar being the first temperature at which we observed primary growth in the E form, and the low temperature of the bar the last temperature at which growth in the 1F form was observed. At high concentrations there is only a small dependence on the transition temperature with concentration, while at lower concentrations the dependence is stronger.

We believe that the observed variation in “transition” temperature with concentration occurs because of concentration/growth rate effects. The concentration dependence of growth rate is expected to be different in the different crystal forms (e.g. 1F and E). The temperature at which 1F material is first seen would then be the temperature at which the 1F form is first able to crystallize more rapidly than the E form (this question of growth rates of competing phases is laid out in detail in Appendix II of Ref. [11]). If the growth rate of the 1F form depends more strongly on concentration than

that of the E form, then the temperature of the cross over from 1F to extended growth will be lower at lower concentrations. Of course the actual cross over temperature will depend on both the supercooling and concentration dependence of the different growth rates. It is generally found that the supercooling dependences of 1F and E growths are different [12]. The exact nature of the concentration dependence of growth rate cannot be obtained from DSC data alone, as this only gives the overall crystallization rate. A comparison of the growth rate data presented here and that in Ref. [6] clearly shows that the concentration dependence of the crystallization rate is considerable.

An alternative, but less likely, explanation is that the highest temperature at which primary growth is observed in the 1F form could be strongly related to the dissolution temperature of that form, with the dissolution temperature varying with concentration, in the “classical” manner observed in small molecules. However, we have found in $C_{198}H_{398}$ that the dissolution temperature is independent of concentration at high dilutions [13], and yet in that alkane the maximum temperature at which 1F crystals can be grown is strongly concentration dependent, in a very similar manner to that shown for $C_{246}H_{494}$ here. As a result we feel that the concentration/growth rate explanation is the correct one.

The above discussion of the relationship between concentration and the cross over from 1F to E growth is of particular importance when we consider the crystal morphologies. Although the exact concentration of a particular sample could be determined by weighing after the DSC pan was sealed, it was not possible to control this concentration exactly, as such small quantities of both toluene and alkane were involved and because of the volatile nature of the solvent. The rate data shown in Fig. 1 were all obtained using a single sample, thus ensuring the constancy of the concentration.

However, in the work to follow where we have examined morphologies, a different sample must be used for each experiment. Thus it becomes impossible to ensure all the concentrations for all the samples (and hence morphologies) are identical. In practice the actual concentration varied from 0.2 to 0.55% in the samples used for the morphological studies, all these concentrations were higher than the concentration used for the DSC study reported above because the yield, from 0.14% w/w was too low. This in turn leads to a variation in the transition temperatures between growth in the different forms. We have therefore carefully recorded the DSC traces for each sample and hence, from the position of the crystallization and melting peaks, determined the actual form in which each is crystallized, etc.

3.1.1. On the unthickened morphologies

For $C_{246}H_{494}$, crystallization in the extended form is, at the high dilutions studied, exceptionally slow, so that it is not convenient to use the DSC to prepare such crystals.

Accordingly, experiments on the crystal morphologies prior to thickening, and at temperatures where thickening did not occur, were primarily performed in glassware in oil baths. For the sake of consistency, comparative crystallization at lower temperatures was performed both in glassware in oil baths and in the DSC. Prior to thickening, the morphologies observed in both sets of experiments were the same, as expected.

Fig. 4 shows a series of TEM micrographs illustrating the different morphologies observed at different crystallization temperatures. At high temperatures long, thread like crystals were generally found (Fig. 4a). In some cases somewhat wider crystals appeared to consist of several of these thread like crystals. On quenching from the crystallization temperature to room temperature, the thread like crystals are often extensively decorated by more folded crystals. From the decoration pattern it seems likely that the original thread like crystals were twins with exceptionally rapid growth due to the re-entrant corner. At lower temperatures, but where primary growth is still in the extended form, a second morphology is also seen, similar to that found in extended chain $C_{198}H_{398}$ [14]; this consists of multiple twins — see Fig. 4b. At this temperature there are also occasional large expanses of extended chain crystals with multiply faceted edges.

As the temperature is lowered further, until primary growth occurs in the 1F form, a different but very distinctive morphology is observed — Fig. 4c. Rectangular twins, as revealed by electron diffraction, in which the twin boundary passes down the long axis of the crystal (the end of the crystal illustrated has broken off, so the re-entrant corner is missing), were almost exclusively found.¹ This morphology is very similar to that found at the highest temperatures of once-folded growth in $C_{198}H_{398}$ [14]. Again, these crystals have grown very extensively in the direction of the re-entrant corner, suggesting a nucleation limited growth process. At somewhat lower temperatures a similar morphology is generally found but with distinctive truncated lozenge type overgrowths. At this temperature very large, lozenge shaped aggregates were also frequently observed. (Some further examples of initial morphologies can be seen in Figs. 5b and 6b, they will be discussed below.)

3.2. Isothermal thickening

Two parallel sets of experiments on isothermal thickening were performed, one in glassware in oil baths — a continuation of the study above — and the other using samples crystallized in DSC pans, continuing the methods used in the previous paper [4]. The most exhaustive study

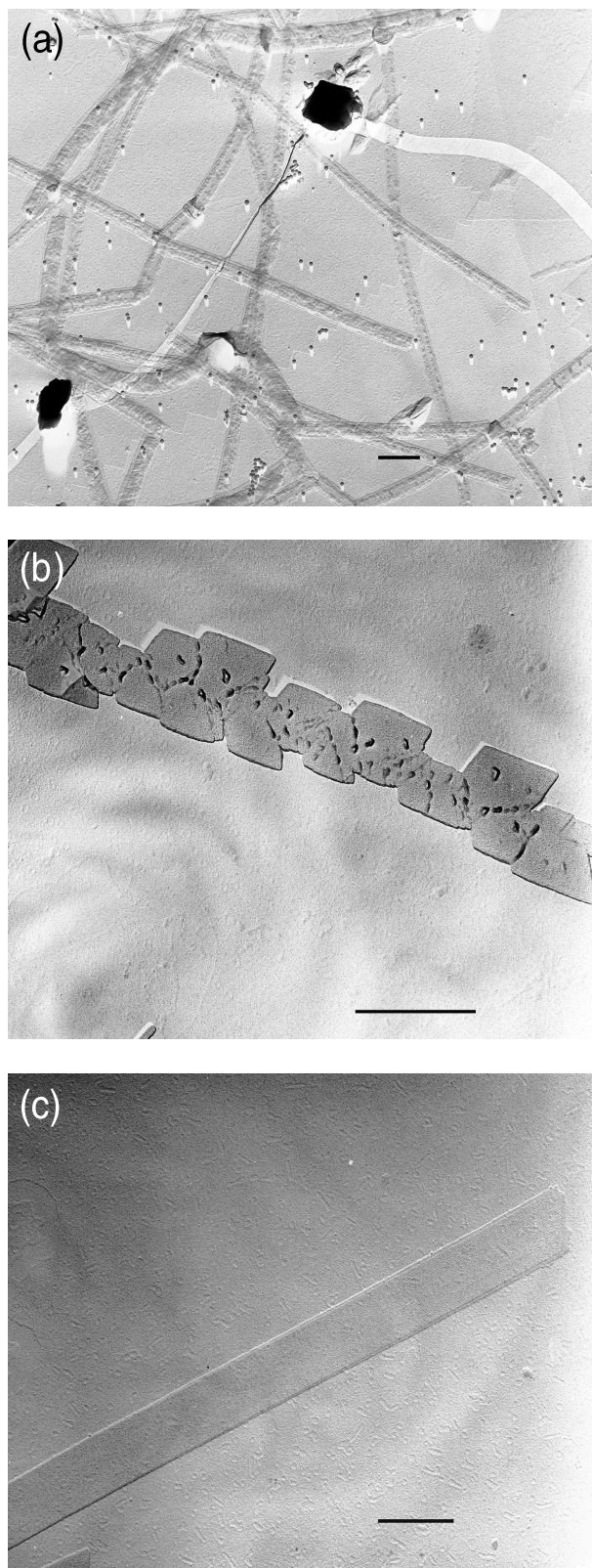


Fig. 4. A series of TEM micrographs showing $C_{246}H_{494}$ crystals crystallized at different temperatures in glass tubes in oil baths, from $\sim 0.2\%$ solution: (a) 89°C ; (b) 85°C ; and (c) 80°C . The crystals grown at 89°C are the prominent lathe like objects in (a). Note that at 89°C the growth rate is very slow leaving much material to crystallize on quenching. Such material can be seen as small overgrowths on the lathe like crystals and as some large lozenge crystals in the background. Scale bars represent $1\ \mu\text{m}$.

¹ It is possible that some readers could (as did one referee) mistake these twin crystals for the remnants of picture frame crystals that could have arisen during the thickening process. We are confident that this is not the case for several reasons: electron diffraction clearly reveals these are twin crystals; in many cases we can see the re-entrant ends of such crystals.

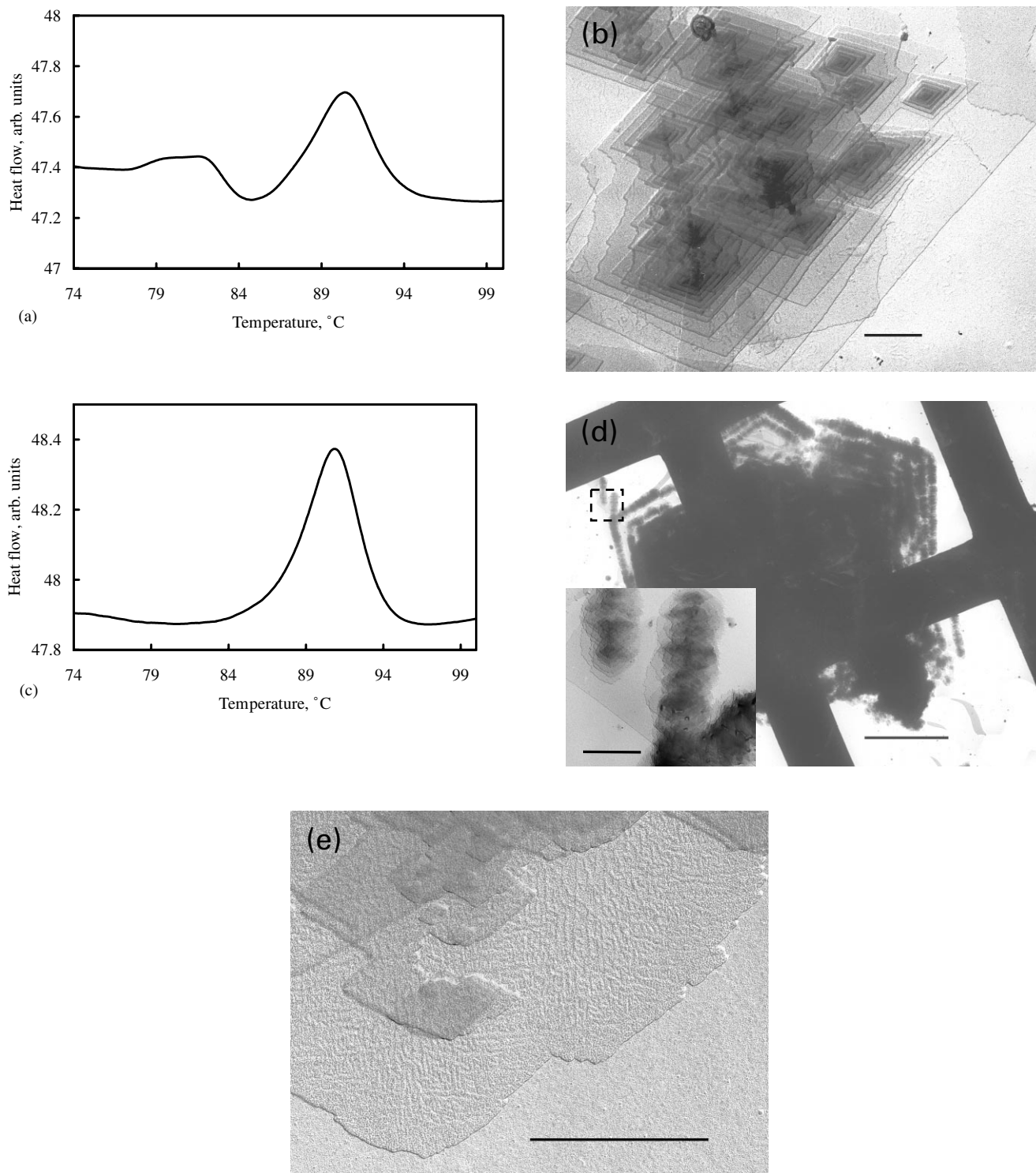


Fig. 5. A series of TEM micrographs and their corresponding DSC traces illustrating thickening from 2F to 1F in $C_{246}H_{494}$. (a) The DSC trace corresponding to (b). The sample was crystallized for 5 min at 74°C. Note the double melting peak which is indicative of thickening during heating in the DSC. (b) A TEM micrograph showing the unthickened 2F morphology. (c) The DSC trace corresponding to Figs. 4d–e. The sample was crystallized for 10 min at 74°C. (d) A low magnification image showing the preferential thickening around the edges of a large aggregate (the scale bar in this image represents 10 μm), inset: a higher magnification image showing screw dislocation overgrowths associated with the thickening. (e) A high magnification image in which the fine scale roughness characteristic of the thickening process can be seen. Scale bars represent 1 μm except for the main part of (d) where the scale bar represents 10 μm .

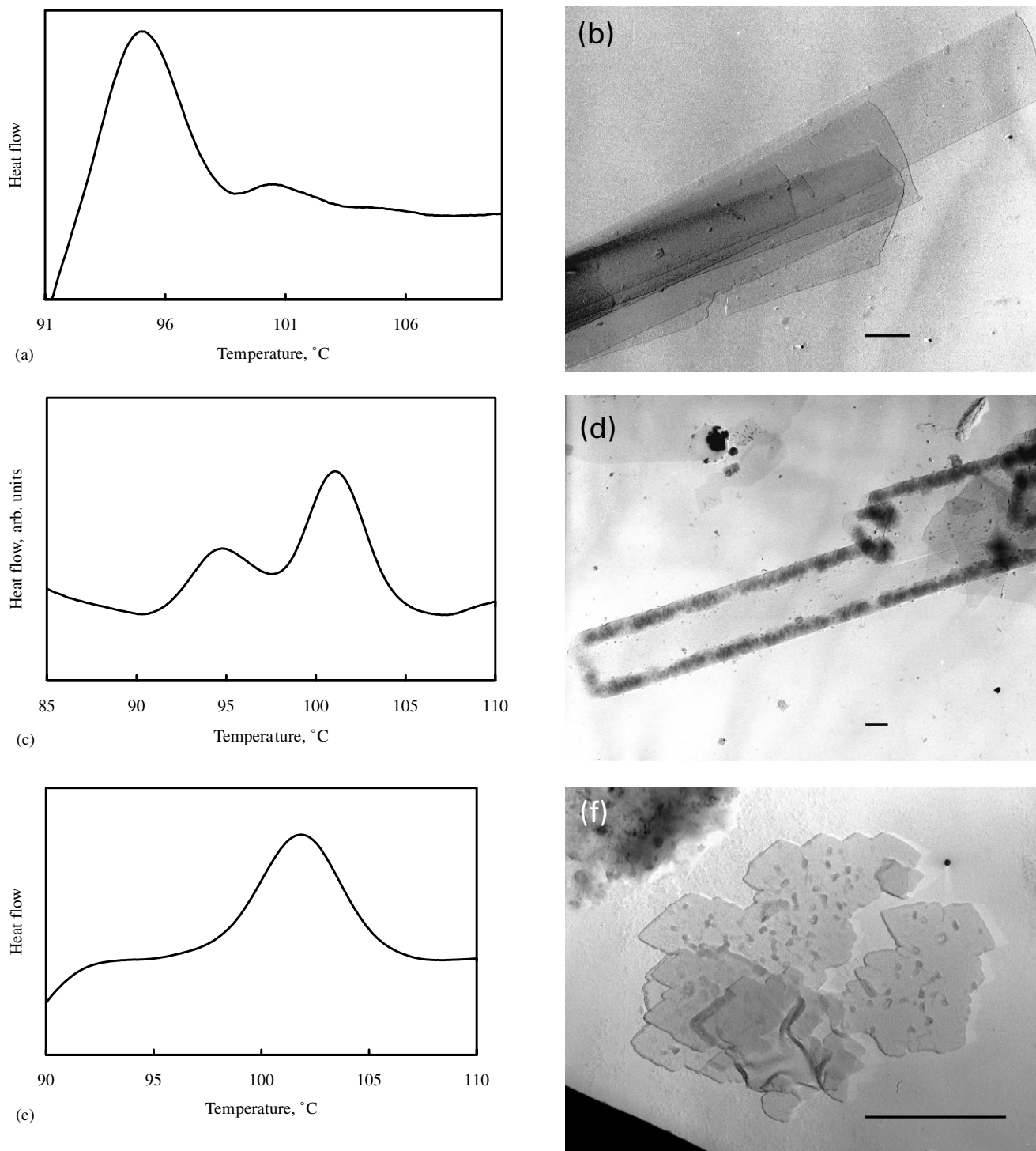


Fig. 6. A series of TEM micrographs and their corresponding DSC traces illustrating thickening from 1F to E in $C_{246}H_{494}$. (a) The DSC trace corresponding to (b). The sample was crystallized for 21 h at 83°C . (b) A rectangular twin characteristic of 1F crystallization at high temperatures. (c) The DSC trace corresponding to (d). The sample was crystallized for 8 h at 83°C . (d) A large rectangular twin with screw dislocation overgrowths around its perimeter. (e) The DSC trace corresponding to (f). The sample was crystallized for 48 h at 83°C . (f) An aggregate of fully thickened material consisting of multiple twins made up of small lozenge shaped crystals. Scale bars represent $1\ \mu\text{m}$.

was done in DSC pans so we shall detail that first, only looking at the study in glassware in cases where, to our initial surprise, the results were significantly different from those in the DSC.

3.2.1. Twice-folded to once-folded-crystallization in DSC

Fig. 5 shows a series of TEM micrographs of unthickened, partially thickened and fully thickened material showing the isothermal transformation from 2F to 1F material in

$C_{246}H_{494}$, and the corresponding DSC traces taken from each sample before it was harvested for TEM examination. Fig. 5a shows the DSC trace corresponding to Fig. 5b, which is of unthickened material. Fig. 5c shows the DSC trace corresponding to Fig. 5d and e, which show partially thickened material. When sufficiently long crystallization times were used, so that most of the material would have crystallized at the isothermal temperature, two separate crystal populations were seen, one consisting of unthickened material and the other consisting of thickened material.

The initial, unthickened morphology (Fig. 5b) is clearly lozenge shaped crystals bound by 110 faces. In many cases these are very heavily multi-layered, giving macroscopic crystals similar to those found in $C_{294}H_{590}$ [4]. (At this short crystallization time the sample would not have been able to crystallize fully, so much of the material will have crystallized during quenching to room temperature.) Fig. 5d shows a very large aggregate of partially thickened material, that originally consisted of multiple lozenge shaped crystals. It can be seen that the edges of the lozenges have preferentially thickened, making rough picture frame type shapes. The inset to Fig. 5d shows a thickened region where the level of multi-layering is not so high, allowing the underlying morphology to be clearly seen. The thickened material consists of approximately lozenge shaped crystals which occur in aggregates apparently growing from a central screw dislocation. These screw-dislocation-born lozenges are almost exclusively oriented in such a way that they appear to be 110 twins with the initial crystal form. The long axis of the lozenge lies approximately perpendicular to the original 110 face of the parent crystal. These spiral growth terraces appear to be related to the thickening process and resemble the screw dislocation growth reported previously [15] during the non-isothermal crystallization of polyethylene.

As crystallization proceeds in the 2F form, the solution concentration is reduced, and at these temperatures we may postulate that the concentration of the transition between primary growth in the 2F and in the 1F form is approached. The resulting competition between different crystal forms (or polymorphs) may be regarded as being similar to an impurity slowing down the growth process [8], and it is often found in polymers that the presence of impurities leads to an increase in the number of screw dislocations. Any such dislocations would be prime sites for thickening to occur as they will be tightly multi-layered. Thus we envisage that primary growth still occurs in the 2F form, but competition with the 1F form leads to the formation of many screw dislocations making these areas particularly susceptible to thickening and leaving approximately crystallographic thickened morphologies.

The majority of the thickened material is found in the small, spiral growth aggregates described above. However, in some areas larger expanses of thickened material are seen which are not bound by a clear crystal face, such as that shown in Fig. 5e, and these often supply a supporting layer

to the overgrowths described above. A finer scale structure is particularly visible on these large, flat regions of thickened material, although closer inspection of the lozenge shaped spirals reveals a similar underlying texture. All the thickened areas have a fine scale roughness with characteristic width of about 10 nm. In some regions individual thickened ribbons are visible in a matrix of apparently unthickened material (such as in Fig. 5e). These thickened regions are interconnected in a complex structure, which, in a similar manner to the “dendritic” structures observed on thickening $C_{294}H_{590}$ [4], appear to follow preferred directions within the crystal (in this case 100 and 010 planes).

The majority of the thickened material does not contain an underlying matrix of unthickened material, but still maintains a small length scale roughness which can be considered as typical of the thickening process from 2F to 1F material. This small length scale roughness is clearly visible in the higher magnification image shown in Fig. 5e. The edges of thickened crystals exhibit a roughness on a similar length scale. In contrast to the thickening behaviour of $C_{294}H_{590}$ between the 2F and 1F form, gaps are not commonly seen between the fine features, but rather they form continuous layers.

3.2.2. Once-folded to extended thickening, crystals prepared in DSC pans

Fig. 6 shows a series of micrographs and their corresponding DSC traces, showing the isothermal thickening behaviour of $C_{246}H_{494}$ as it transforms from 1F to E material. Fig. 6a shows the DSC trace corresponding to Fig. 6b, in which no thickening has occurred. Fig. 6c shows the DSC trace corresponding to Fig. 6d in which partial thickening has occurred. Fig. 6e shows the DSC trace corresponding to Fig. 6f, the crystal in the figure is entirely thickened. The initial, unthickened morphology, was a rectangular crystal, Fig. 6b (note the morphology here is similar to that seen in Fig. 4c where the crystals were grown in glassware in the oil bath). As thickening proceeds, as shown by the evolution of the DSC peak from the extended form, an overgrowth layer starts to form along the outer edges of the rectangular crystals. With progressive thickening this layer becomes thicker (i.e. more multi-layered). Finally, once the DSC shows exclusively thickened material remaining, a morphology apparently unrelated to the parent morphology is left.

Parallel studies, measuring the thickness of these crystals using Raman LAM [16] have shown that the partially thickened material, as shown by DSC, does indeed contain both unthickened and extended chain material. The overgrowths themselves resemble the screw dislocation based thickened overgrowths seen after the transformation from 2F to 1F material. However, in the present case at least, the outer rim of each crystal has not yet thickened — it must be assumed that within the overgrowth a core of extended chain material exists.

In the totally thickened morphology shown in Fig. 6f the outer edges of the thickened crystals are relatively clean

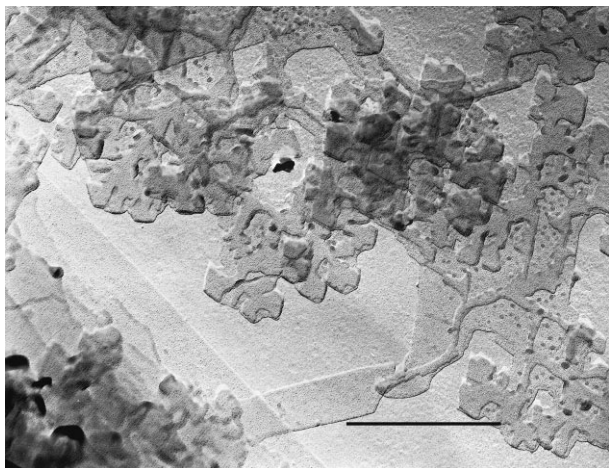


Fig. 7. An electron micrograph showing crystals grown in glassware in oil baths at 80°C for 55 h at a concentration of ~0.2%. The scale bar represents 1 μm .

crystallographic faces, although the points are somewhat blunted. Thickening in this case is clearly accompanied by the deposition of new material from the solution. Initial growth is of isolated, rectangular, 110 twins. After these have grown to considerable size, they start to form screw dislocations at their edges which facilitate the subsequent thickening into the extended form, possibly in a similar manner to that suggested to occur on thickening from the 2F to the 1F form. These overgrowths grow in the *c*-axis direction as well as spreading laterally across the surface of the parent crystal. It appears that, at least in some cases, these overgrowths are rotated with respect to the crystallography of the parent crystal. At very long times all of the folded material is cannibalized by the extended chain crystals, leaving a crystal population of almost exclusively extended chain crystals. As no isolated remnants of partially thickened material were found at long times, it is safe to assume that extensive dissolution and re-crystallization has occurred.

3.2.3. Once-folded to extended thickening, crystals prepared in oil baths

The above morphologies were seen on thickening from 1F to E material in DSC pans. Parallel experiments were also performed in glassware in oil baths. Fig. 7 shows an example of a partially thickened crystal. There are many approximately lozenge shaped areas of thickened material. This image is strikingly similar to the thickening seen in $\text{C}_{198}\text{H}_{398}$ between the 1F and E forms shown in Fig. 7 in Ref. [2]. Comparing Figs. 6d and 7, (both showing partially thickened material) it is apparent that there are differences between the resultant morphologies and thickening mechanisms from those prepared in DSC pans and those in glassware in oil baths, although the initial crystal forms are the same. Note, in particular, that from the DSC we find crystals with thickening around the edges (Fig. 6d), while from the

oil bath we find thickening throughout the whole crystal (Fig. 7).

It is clear that the thickening route found when crystallization is carried out in glassware in oil baths is significantly different from that found when crystallization is performed in aluminium pans in the DSC. In our view this is because the experiments performed in glassware are almost certainly not strictly isothermal. We would expect a very shallow temperature gradient to exist within the solution, and there may be occasional small fluctuations in the temperature of the bath. During the long crystallization period the thickening process may well be nucleated when a crystal is temporarily hotter than the average temperature of the bath. This thickened region would then spread through the rest of the crystal, but result in a different morphology from that seen in the DSC experiment.

It is also possible that different thickening mechanisms can be facilitated by the presence of different surfaces in the different vessels (aluminium in the DSC and glass in the other case). However, the similar initial morphologies are hard to reconcile with such a view.

Finally, the different morphologies might be related to the difference in nucleation rates in the two different types of vessel. In glassware thickening experiments were carried out at lower temperatures than those used in DSC pans, and the samples were held for considerably longer times, as the initial rate of nucleation was slow. The difference in thickened morphologies may therefore be a combination of the increased amount of material left in solution at long times in the glass vessel and the presence of small fluctuations in temperature facilitating the onset of thickening.

4. Conclusions

The crystallization and isothermal thickening behaviour of $\text{C}_{246}\text{H}_{494}$ have been studied using DSC and TEM. Using DSC a minimum in crystallization rate has been found at the transition from primary growth in the 2F form to the 1F form, and another at the transition from growth in the 1F form to the extended form. The temperature of the transition between different folded forms has been found to depend strongly on solution concentration, particularly at low concentrations.

We suggest that for comparison between morphologies and rates measured in the DSC, it is essential to grow the crystals in the DSC. Even quite small variations in concentration can lead to significant differences in the temperatures at which the different crystal forms grow, making it essential to have direct DSC data available to identify the actual crystal forms present unambiguously.

A number of different morphologies have been identified for primary growth at different crystallization temperatures. When isothermal thickening is carried out between 2F and 1F crystals, a thickening morphology is observed

characterized by preferential thickening at crystal edges following screw dislocation growth, with a fine scale roughness on the scale of tens of nanometres. We propose that the fine scale roughness is caused by competition between the thickening process and the strain it induces in the crystal lattice. We suggest that the screw dislocation growth at the edges of the crystals is the result of competition between 2F and 1F polymorphs. In the DSC, thickening from 1F to E is again found to initiate at the edges of the crystals, following the formation of screw dislocations. However, in this case the final thickened morphology does not contain the roughness observed on thickening between different folded forms, and bears no resemblance to the initial, unthickened morphology. We suggest that in this case considerable rearrangement must occur, possibly accompanied by some dissolution and re-deposition of material.

Acknowledgements

We would like to thank the EPSRC (grant no. GR/L07482) for financial support for this work, and G. Brooke and the EPSRC for providing the alkanes. We would also like to acknowledge the significant contribution made to this work by the late Prof Andrew Keller. In our frequent discussions during the course of the work presented here, his knowledge and enthusiasm were an inspiration.

References

- [1] Brooke GM, Burnett S, Mohammed S, Proctor D, Whiting MC. Versatile process for the syntheses of very long chain alkanes, functionalised derivatives and some branched chain hydrocarbons. *J Chem Soc — Perkin Trans 1* 1996;13:1635.
- [2] Organ SJ, Ungar G, Keller A. Isothermal refolding in crystals of long alkanes in solution. II. Morphological changes accompanying thickening. *J Polym Sci Part B: Polym Phys* 1990;28:2365.
- [3] Ungar G, Organ SJ. Isothermal refolding in crystals of long alkanes in solution. 1. Effect of surface self-poisoning. *J Polym Sci Part B: Polym Phys* 1990;28:2353.
- [4] Hobbs JK, Hill MJ, Barham PJ. Isothermal thickening of single crystals of $C_{294}H_{590}$ in dilute solution. *Polymer* 2000;41:8761.
- [5] Organ SJ, Ungar G, Keller A. Rate minimum in solution crystallization of long paraffins. *Macromolecules* 1989;22:1995.
- [6] Organ SJ, Barham PJ, Hill MJ, Keller A, Morgan RL. A study of the crystallization of the *n*-alkane $C_{246}H_{494}$ from solution: further manifestations of the inversion of crystallization rates with temperature. *J Polym Sci B: Polym Phys* 1997;35:1775.
- [7] Morgan RL, Barham PJ, Hill MJ, Keller A, Organ SJ. The crystallization of the *n*-alkane $C_{294}H_{590}$ from solution: inversion of crystallization rates, crystal thickening, and effects of supersaturation. *J Macro-Sci Phys* 1998;37:319.
- [8] Ungar G, Keller A. Inversion of the temperature dependence of crystallization rates due to onset of chain folding. 1987;28:1899.
- [9] Organ SJ, Keller A, Hikosaka M, Ungar G. Growth and nucleation rate minima in long *n*-alkanes. 1996;37(12):2517.
- [10] Boda E, Ungar G, Brooke GM, Burnett S, Mohammed S, Proctor D, Whiting MC. Crystallization rate minima in a series of *n*-alkanes from $C_{194}H_{390}$ to $C_{294}H_{590}$. *Macromolecules* 1997;30(16):4674.
- [11] Keller A, Hikosaka M, Rastogi S, Toda A, Barham PJ, Goldbeck-Wood G. An approach to the formation and growth of new phases with application to polymer crystallization — effect of finite-size, metastability, and Ostwald rule of stages. *J Mater Sci* 1994;29(10):2579.
- [12] Hoffman JD. Growth rate of extended-chain crystals: the lateral surface free energy of pure n - $C_{94}H_{190}$ and a fraction $\sim C_{207}H_{416}$. *Macromolecules* 1985;18:772.
- [13] Hobbs JK, Hill MJ, Keller A, Barham PJ. Experimentally determined temperature-concentration phase diagrams of monodisperse alkanes with chains containing between 100 and 200 carbons. *J Polym Sci B: Polym Phys Ed* 1999;37:3188.
- [14] Organ SJ, Keller A. The onset of chain folding in ultralong *n*-alkanes: an electron microscopic study of solution-grown crystals. *J Polym Sci B: Polym Phys* 1987;25:2409.
- [15] Bassett DC, Keller A. On the habits of polyethylene crystals. *Philos Mag* 1962;7:1553.
- [16] Hobbs JK, Hill MJ, Barham PJ, Dosiere M (in preparation).